0021-972X/90/7003-0661$02.00/0
Journal of Clinical Endocrinology and Metabolism

Vol. 70, No. 3
Printed in U.S.A.

Evaluation of Receptors for Somatostatin in Various Tumors Using Different Analogs*

GORDAN SRKALOVIC, REN-ZHI CAI, and ANDREW V. SCHALLY

Endocrine, Polypeptide, and Cancer Institute, Veterans Administration Medical Center, and the Department of Medicine, Tulane University Medical School, New Orleans, Louisiana 70146

ABSTRACT. The binding characteristics of several somatostatin (SS-14) analogs developed in our laboratory were examined in various human and animal tumors and normal tissues. In rat cerebral cortex and human breast cancer membranes the interaction of SS-14 with its binding sites was rapid, specific, saturable, linear with protein concentrations, and dependent on time and temperature. Analysis of kinetic and equilibrium experimental data showed that the interaction of [^{125}I-Tyr^{11}]SS-14 with the binding sites in all normal and tumoral tissue specimens was consistent with the presence of a single class of noncooperative binding sites. Superactive octapeptide analogs of somatostatin-containing hexapeptide sequences Cys-Phe-D-Trp-Lys-Thr-Cys or Cys-Tyr-D-Trp-Lys-Val-Cys showed significant binding affinities to SS-14 receptors. Among these analogs, D-Trp-Cys-Phe-D-Trp-Lys-Thr-Cys-Thr-NH_2 (RC-98-I) showed the highest binding affinity to normal human pancreatic tissue and human pancreatic adenocarcinoma. In contrast, Sandostatin (SMS 201-995) bound only to normal pancreas, not to human pancreatic cancers. Analog RC-98-I also showed a high binding to human and rat prostate cancers. In human epithelial ovarian cancers and an arrhenoblastoma, analogs D-Phe-Cys-Phe-D-Trp-Lys-Thr-Cys-Trp-NH_2 (RC-95-I), D-Phe-Cys-Tyr-D-Trp-Lys-Val-Cys-Thr-NH_2 (RC-121) and D-Phe-Cys-Tyr-D-Trp-Lys-Val-Cys-Trp-NH_2 (RC-160) appeared to be the most potent in displacing labeled SS-14. Analogs Ac-Phe-Cys-Phe-D-Trp-Lys-Thr-Cys-Thr-NH_2 (RC-101-I) as well as RC-121, RC-160, and RC-95-I, but not SMS-201-995, showed high binding affinity in human breast cancers. In specimens of human meningioma the highest binding was found with analogs RC-121, RC-95-I, and RC-101-I. Since marked variations in binding affinities were noted for several analogs in the tissues of origin and the tumors, this suggests that differences may exist between somatostatin receptors not only in normal *vs.* cancerous tissues, but also among various tumors. Our findings also imply that some analogs could be therapeutically superior to others in the treatment of certain tumors. (*J Clin Endocrinol Metab* **70:** 0000, 1990)

SOMATOSTATIN has many biological actions, inhibits a large variety of cells, and appears to be an endogenous antiproliferative agent (1–4). Various studies demonstrated inhibitory effects of somatostatin in patients with acromegaly, endocrine pancreatic tumors such as insulinomas and glucagonomas, and ectopic tumors such as gastrinomas and vasoactive intestinal peptide-producing tumors (1, 2, 5–8). However, the half-life of somatostatin is very short, so that its therapeutic use is impractical (1, 5, 6). Several groups, including ours, designed and synthesized somatostatin analogs with more selective and prolonged activities (1, 5, 6, 9–12).

Because of a wide spectrum of activities, including suppression of the secretions of the pituitary, pancreas, stomach, and gut, interference with growth factors, and possible direct antiproliferative effects on some tissues, somatostatin analogs might inhibit various tumors through multiple mechanisms (1–5, 12–14). Direct antiproliferative actions of somatostatin analogs are most likely mediated by specific receptors located on tumor cells. High affinity binding sites for somatostatin and its analogs have been found in normal tissues and in tumors (2, 6, 12).

Previously, we demonstrated inhibitory effects of our analogs RC-121 and RC-160 on the growth of prostate, breast, and pancreatic cancers (4, 15, 16). Our other octapeptide analogs were also designed for antitumor activity (10, 11). In the course of detailed studies on these new peptides, we analyzed their receptor-binding characteristics in an attempt to select the most suitable analog for the treatment of tumors originating from different tissues. Since it is possible that distinct somatostatin receptors are expressed in the normal *vs.* cancerous cells (17), we performed binding studies on various normal tissue and tumor specimens obtained from humans and experimental animals. The present report gives an account of our work.

Received August 7, 1989.
Address all correspondence and requests for reprints to: Dr. Andrew V. Schally, Veterans Administration Medical Center, 1601 Perdido Street, New Orleans, Louisiana 70146.
* This work was supported by NIH Grants CA-40003, CA-40004, and CA-40077; the Medical Service of the V.A.; the G. Harold and Leila Y. Mathers Foundation; and the U.S. Cancer Research Council (to A.V.S.).

Materials and Methods

Peptides

Somatostatin-14 (SS-14) and [Tyr[11]] SS-14 were provided by Debiopharm S.A. (Lausanne, Switzerland). SMS-201-995 (D-Phe-Cys-Phe-D-Trp-Lys-Thr-Cys-Thr-OL) (9) was kindly provided by Sandoz Ltd. (Basel, Switzerland). Octapeptide analogs of SS-14 shown in Table 1 were synthesized using standard solid phase procedures and purified by high pressure liquid chromatography (HPLC), as previously reported (10, 11).

Buffers

The homogenization buffer consisted of 0.3 M sucrose, 25 mM Tris base, 0.25 mM phenylmethylsulfonylfluoride, 1 mM EGTA, 10 mM monothioglycerol and Trasylol (aprotinin) at 10,000 kallikrein inactivator units/liter (pH 7.5). Receptor binding of SS-14 was carried out in 50 mM Tris base, 5 mM $MgCl_2$, 0.2% BSA, Trasylol (100,000 U/liter), bacitracin (20 mg/L), and 0.25 mM phenylmethylsulfonylfluoride (pH 7.5). The wash buffer was the same as assay buffers, but did not contain BSA. The chemicals used for buffers were purchased from Sigma Chemical Co. (St. Louis, MO).

Preparation of membranes

Normal tissues from experimental animals were obtained from adult female and male Sprague-Dawley rats (Charles River Breeding Laboratories, Wilmington, MA) and Syrian golden hamsters (NCI, Frederick Cancer Research Facility, Frederick, MD). R-3327H Dunning rat prostate adenocarcinoma were provided by Dr. Norman Altman (Papanicolaou Cancer Research Institute, Miami, FL) (4, 18). Pancreatic cancers in hamsters were induced with N-nitrosobis-(2-oxopropyl)-amine (BOP) as previously described (15). Normal human specimens were obtained from Laboratory Services of the V.A. Medical Center (New Orleans, LA). Autopsies were performed 6–18 h after death. Before completing the receptor assays, all autopsy specimens were carefully examined by our pathologist (Dr. Bela Szende). Only those specimens that did not show signs of postmortem autolysis were selected for receptor studies. The age of patients from whom the normal prostate specimens were obtained ranged from 58–62 yr, and in the case of normal pancreas 64–75 yr. Active normal ovary (premenopausal) was obtained from a 36-yr-old woman, while inactive (postmenopausal) ovary was obtained from a 64-yr-old woman at autopsy.

TABLE 1. The structures of somatostatin analogs synthesized in our laboratory and tested in receptor binding assays

Code	Structure
RC-121	D-Phe-Cys-Tyr-D-Trp-Lys-Val-Cys-Thr-NH_2
RC-160	D-Phe-Cys-Tyr-D-Trp-Lys-Val-Cys-Trp-NH_2
RC-95-I	D-Phe-Cys-Phe-D-Trp-Lys-Thr-Cys-Trp-NH_2
RC-98-I	D-Trp-Cys-Phe-D-Trp-Lys-Thr-Cys-Thr-NH_2
RC-101-I	AcPhe-Cys-Phe-D-Trp-Lys-Thr-Cys-Thr-NH_2

Specimens of human pancreatic adenocarcinoma were obtained from Dr. V. Hollander, Mount Sinai Medical Center (New York, NY). The age of pancreatic cancer patients ranged from 65–69 yr. Human prostate cancers were obtained after radical prostatectomy from Dr. J. E. Pontes, Section of Urologic Oncology, the Cleveland Clinic Foundation (Cleveland, OH). The average prostate cancers Gleason grade was 7 (range, 5–9). The mean age of prostate cancer patients was 64.6 (range, 56–72 yr). Breast cancer specimens were obtained from Dr. J. L. Wittliff after biopsies performed in women, 28–82 yr of age, suspected of having breast cancer. Breast biopsies were performed at James Graham Brown Cancer Center, University of Louisville, School of Medicine (Louisville, KY). Ovarian cancers (poorly differentiated ovarian adenocarcinomas and arrhenoblastoma) were obtained from Dr. Eric L. Jenison (OB/GYN and Gynecologic Oncology and Reconstructive Pelvic Surgery, Akron, OH) and Dr. J. Bellina, the Omega International Institute (New Orleans, LA). The age of ovarian cancer patients was 48–60 yr. Human cancer specimens were frozen and shipped on dry ice to the Endocrine, Polypeptide, and Cancer Institute (New Orleans, LA) for membrane receptor assays. The specimens were stored at −70 C until processed. Cerebral cortex tissue of male Sprague-Dawley rats was used as positive controls for SS-14 binding.

Samples were cleaned of fat and connective tissue, cut into small slices, and homogenized in 5 vol sucrose buffer using an Ultra-Turrax homogenizer (Tissumizer, Tekmar, Cincinnati, OH) at maximal speed 5 for 5-s strokes at 0 C. The homogenate was centrifuged at 500 × *g* for 10 min at 4 C. The supernatant containing the crude membrane fractions was then ultracentrifuged at 70,000 × *g* for 45 min at 4 C (Beckman Preparative Ultracentrifuge, Beckman Instruments, Inc., Palo Alto, CA). The resulting pellet was resuspended in wash buffer and used for the receptor binding studies. Protein concentration was determined by the Bio-Rad protein assay kit (Richmond, CA) according to Bradford (19).

For the radioiodination of [Tyr[11]]SS-14, a modification of the chloramine-T of Greenwood *et al.* (20) method was used. An aliquot of the peptide (5 μg in 5 μl 0.01 N acetic acid) was mixed with 40 μL 0.5 M phosphate buffer and 1 mCi ^{125}I Na in a volume of 2 μL. Ten microliters of chloramine-T were added. The reaction lasted 30 s at room temperature and was stopped by adding 10 μL cysteine (5.1 mg/mL in 0.5 M phosphate buffer) and diluting with 500 μL 0.5 M phosphate buffer. The purification of the labeled peptide was carried out using the HPLC with a C-18 column (W-Porex 5C18, 250 × 4.6 mm id; Phenomenex, Rancho Palos Verdes, CA). The specific activity was 78–141.8 μCi/μg.

The binding assay of SS-14 was conducted as described previously (18, 21). Binding reactions were performed in 12 × 75-mm polypropylene round-bottom culture tubes at 21 C, using a competitive inhibition method. Displacement curves were obtained with 100–140 pM iodinated [^{125}I]SS-14 in the presence of increasing amounts of unlabeled SS-14 (150 pM to

1.5 μM). The procedure was as follows. Fifty microliters of unlabeled SS-14 in incubation buffer and 50 μL labeled ligand were placed into the tube and vortexed, and 50 μL of the suspension containing the membrane receptor fraction were added. In each binding experiment, one set of tubes was used with 50 μL wash buffer instead of membrane to determine the radioactivity bound to nonmembrane particles. Each assay point was performed in triplicate. The tubes were incubated for 120 min at 21 C. The reaction was terminated by rapid filtration through glass fiber filters (Filtermats-Receptor Binding, Skatron, Inc., Lier, Norway), prewetted in assay buffer and presoaked for at least 3 h in 0.5% polyethylenimine solution to minimize filter adsorption. A semiautomatic cell-harvesting system (Skatron) with 10-s washing time was used. The radioactivity of filters was counted in an automatic γ-counter (Micromedic System, Inc., Huntsville, AL). The specificity of SS-14 binding to its receptors was investigated using competitive inhibition studies with labeled SS-14 and unlabeled D-Trp^6-LHRH (160 pM to 1.6 μM) and epidermal growth factor (EGF; 0.1–100 ng).

Mathematical analysis of the binding data

The counts of radioactivity obtained from filters or tubes containing membrane particles were corrected by deducting the background count from assays in which no membranes were added. The Ligand-PC computerized curve-fitting program of Munson and Rodbard (22) was used to determine the types of receptor binding, dissociation constant (K_d), and the maximal binding capacity of receptors (B_{max}). Analysis of kinetic studies was made using a collection of radioligand binding analysis programs by G. A. McPherson (Elsevier-BIOSOFT, Cambridge, United Kingdom).

Results

Binding kinetics

Rat cerebral cortex membranes. As shown in Fig. 1, binding of [^{125}I-Tyr^{11}]SS-14 in rat cerebral cortex membranes was time and temperature dependent. At 21 C, specific binding increased with time to reach maximal values after 120 min of incubation (Fig. 1, A). At 4 C maximal specific binding was also reached after 120 min, but remained below that observed of 21 C. Consequently, all subsequent experiments were performed at 21 C. After reaching equilibrium, binding remained constant for at least an additional 120 min. The rate of ligand binding during association experiments followed pseudofirst order kinetics. Dissociation of [^{125}I-Tyr^{11}]SS-14 from rat cerebral cortex membranes was also dependent on time (Fig. 1, B). The rate of decline of [^{121}I-Tyr^{11}]SS-14 binding followed simple first order kinetics. Calculations of association (K_1) and dissociation (K_{-1}) rate constants gave values of 7.06×10^8 M^{-1} min^{-1} and 0.0195 min^{-1}, respectively. The K_d value from kinetic behavior was calculated as $K_{-1}/K_1 = 2.75 \times 10^{-11}$ M. Data from these kinetic studies suggested that only one class of receptors

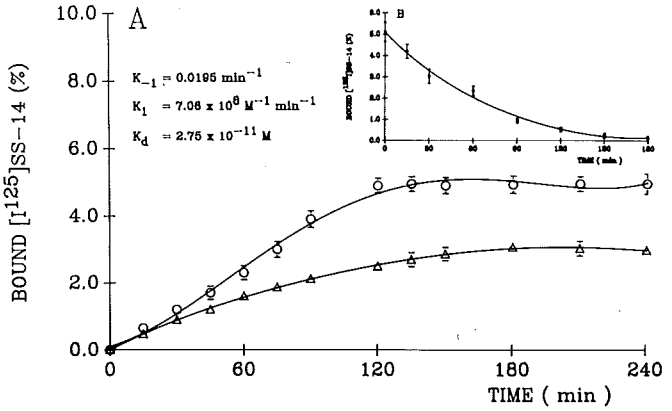

FIG. 1. Association and dissociation kinetics of [^{125}I-Tyr^{11}]SS-14 binding to membranes from rat cerebral cortex. The membranes were incubated in 0.15 mL with 115 pmol [^{125}I-Tyr^{11}]SS-14 for the time intervals indicated in the absence (total binding) and presence (nonspecific binding) of 1.5 μmol unlabeled SS-14. Specific binding represents the difference between total and nonspecific binding. In A the time course of specific binding after incubation at 21 C (○—○) and 4 C (△—△) is represented. In the experiment shown in B, dissociation was initiated by the addition of 3.0 μmol unlabeled SS-14 after 120-min incubation at 21 C. Specific binding (○—○) represents the difference between total and nonspecific binding. All values given represent the extent of binding, expressed as a percentage of the total radioactivity added to each tube. Each *point* is the average value ± SE of triplicate determinations.

for SS-14 is present on rat cerebral cortex membranes.

Rat anterior pituitary and human breast cancer membranes. Specific binding of [^{125}I-Tyr^{11}]SS-14 to membranes of rat anterior pituitary and human breast cancer was also time dependent (Figs. 2 and 3). In both tissues the rate of ligand binding during association experiments followed pseudofirst order of kinetics (Figs. 2A and 3A). Association rate constants (K_1) were 1.43×10^7 M^{-1} min^{-1} for binding to rat anterior pituitary membranes and 3.2×10^7 M^{-1} min^{-1} for binding to human breast cancer membranes. Dissociation rate constants were 0.0145 and 0.0218 min^{-1}, respectively. From kinetic studies K_d values were estimated to be 1.02×10^{-9} M for [^{125}I-Tyr^{11}]SS-14 binding to rat anterior pituitary membranes and 6.81×10^{-10} M for binding to human breast cancer membranes. Monoexponential model was selected as the most appropriate for binding to both rat anterior pituitary membranes and human breast cancer tissue.

Dependence of [^{125}I-Tyr^{11}]SS-14 binding to rat cerebral cortex on plasma membrane concentrations

[^{125}I-Tyr^{11}]SS-14 binding to rat cerebral cortex membranes increased in a linear fashion as a function of plasma membrane protein concentration over a range of 0–200 μg membrane protein in a 0.15-mL incubation volume. Specific binding decreased slightly at higher protein concentrations (200–400 μg), probably due to

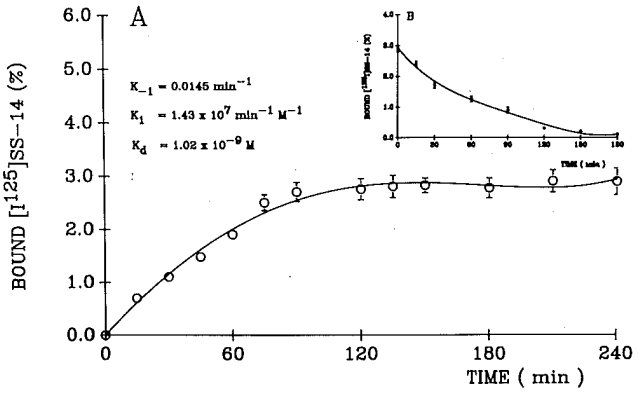

FIG. 2. Association and dissociation kinetics of [^{125}I-Tyr^{11}]SS-14 binding to membranes from rat anterior pituitary. The membranes were incubated in 0.15 mL with 115 pmol [^{125}I-Tyr^{11}]SS-14 at 21 C for the time intervals indicated in the absence (total binding) and presence (nonspecific binding) of 1.5 μmol unlabeled SS-14. Specific binding (O—O) represents the difference between total and nonspecific binding, as indicated in A. In the experiment illustrated in B, dissociation was initiated by the addition of 3.0 μmol unlabeled SS-14 after 120-min incubation at 21 C. Specific binding (O—O) represents the difference between total and nonspecific binding. All values given represent the extent of binding expressed as a percentage of the total radioactivity added to each tube. Each *point* is the average value ± SE of triplicate determinations.

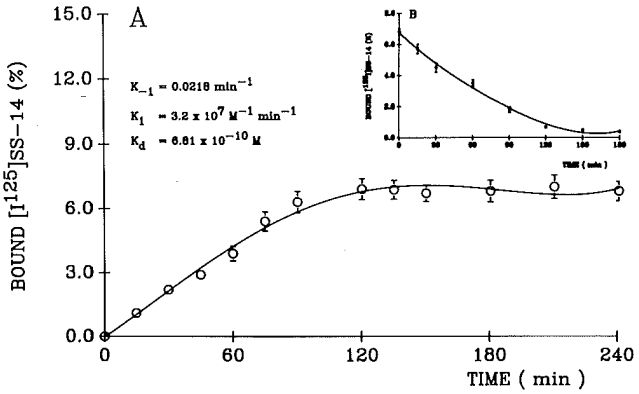

FIG. 3. Association and dissociation kinetics of [^{125}I-Tyr^{11}]SS-14 binding to membranes from human breast cancer specimens. The membranes were incubated in 0.15 mL with 115 pmol [^{125}I-Tyr^{11}]SS-14 at 21 C for the time intervals indicated in the absence (total binding) and presence (nonspecific binding) of 1.5 μmol unlabeled SS-14. Specific binding (O—O) represents the difference between total and nonspecific binding as indicated in A. In the study shown in B, dissociation was initiated by the addition of 3.0 μmol unlabeled SS-14 after 120-min incubation at 21 C. Specific binding (O—O) represents the difference between total and nonspecific binding. All values given represent the extent of binding expressed as a percentage of the total radioactivity added to each tube. Each *point* is the average value ± SE of triplicate determinations.

increasing dissociation of labeled [^{125}I-Tyr^{11}]SS-14. Therefore, plasma membrane protein concentrations of 30–100 μg in a 0.15-mL incubation volume were used in subsequent experiments.

Comparison of affinities of SS-14 and its analogs to membrane receptors in various normal and tumoral tissues

The analysis of displacement curves of [^{125}I-Tyr^{11}]SS-14 by unlabeled SS-14 in all tissue specimens investigated suggested that the labeled SS-14 was bound to one class of noncooperative binding sites. Binding of [^{125}I-Tyr^{11}]SS-14 to different tissue specimens was specific, since unlabeled D-Trp^6-LHRH (160 pmol to 1.6 μmol) and EGF (0.1–100 ng) were unable to displace labeled SS-14 from its binding sites.

Homologous displacement assay of [^{125}I-Tyr^{11}]SS-14 by unlabeled SS-14 in rat cerebral cortex revealed that the labeled peptide was bound to one class of binding sites with high affinity (K_d = 2.7 × 10^{-11} M) and low capacity (B_{max} = 1.95 × 10^{-14} mol/mg membrane protein). When various somatostatin octapeptide analogs were examined in heterologous displacement assay, RC-121 and RC-95-I showed the highest affinity to receptors for SS-14 in rat cerebral cortex membranes (Table 2). In this tissue, SMS-201-995 showed 2 times less affinity than SS-14 and about 16 times less affinity than RC-121 and RC-95-I.

In membranes from human meningioma specimens, the highest affinities for SS-14 receptors were shown by RC-101-I and RC-95-I, as based by displacement of [^{125}I-Tyr^{11}]SS-14 in heterologous assays (Table 2). In these experiments the affinities of RC-101-I and RC-95-I were 92 and 44 times higher, respectively, than that of SS-14.

In normal human pancreas and human pancreatic cancer specimens, analysis of homologous displacement of [^{125}I-Tyr^{11}]SS-14 by unlabeled SS-14 suggested that the labeled peptide was bound to one class of low capacity binding sites with B_{max} values of 4.5 × 10^{-14} and 2.7 ×

TABLE 2. Displacement of [^{125}I-Tyr^{11}]SS-14 with SS-14 and its analogs from rat cerebral cortex and human meningioma membrane receptors

Tissue	Peptides (unlabeled)	K_a (nM^{-1})
Rat cerebral cortex	SS-14	36.41
	RC-121	296.38
	RC-160	4.78
	RC-95-I	292.04
	RC-98-I	ND
	RC-101-I	23.21
	SMS-201-995	17.6
Human meningioma	SS-14	6.55
	RC-121	24.88
	RC-160	3.98
	RC-95-I	287.34
	RC-98-I	3.36
	RC-101-I	598.78

K_a, Affinity constant of ligand for membrane receptors; ND, no displacement. The results of each experiment were calculated from data of triplicate tubes of a 10-point assay. The coefficients of variations of the determinations ranged from 10–30%.

10^{-13} mol/mg membrane protein, respectively. The affinity in pancreatic cancers ($K_d = 3.5 \times 10^{-9}$ M; Fig. 4) was lower than that in normal pancreas ($K_d = 2.9 \times 10^{-9}$ M). Analog RC-98-I was highly potent in displacing [^{125}I-Tyr^{11}]SS-14 from membranes of both normal and carcinomatous pancreatic tissue (Table 3). SMS-201-995 showed high affinity to SS-14 receptors in normal human pancreatic tissue, but its affinity to receptors in human pancreatic cancers was very poor (288 times less than SS-14). In the MIA PaCa-2 human pancreatic cancer cell line heterologous displacement assays showed that RC-98-I and RC-160 had the highest affinities for SS-14 receptors. As can be seen in Table 3, labeled SS-14 was also bound to normal pancreas and BOP-induced pancreatic cancer in Syrian hamsters. Among the analogs investigated, RC-121 showed the highest potency for displacing [^{125}I-Tyr^{11}]SS-14 from its binding sites on BOP-induced pancreatic cancer membranes. However, the affinities of RC-121 and other analogs for SS-14 receptors on BOP-induced cancer membranes were much lower than that of SS-14 (Table 3).

The displacement of [^{125}I-Tyr^{11}]SS-14 from binding sites in membranes of normal human prostate and human prostate cancer specimens by increasing concentrations of unlabeled SS-14 and Scatchard analysis of these data suggested that in both cases the labeled peptide was bound to one class of binding sites. However, in normal prostate we found receptors with low affinity ($K_d = 1.4 \times 10^{-8}$) and high capacity ($B_{max} = 1.5 \times 10^{-12}$) and in prostate cancer, high affinity ($K_d = 4.0 \times 10^{-10}$) and low capacity ($B_{max} = 1.4 \times 10^{-14}$ mol/mg membrane protein; Fig. 5). Among the analogs tested, RC-121 showed the highest affinity for SS-14-binding sites on membranes of normal human prostate (Table 4). Affinity of SS-14 for its receptors on normal human prostate was 95 times

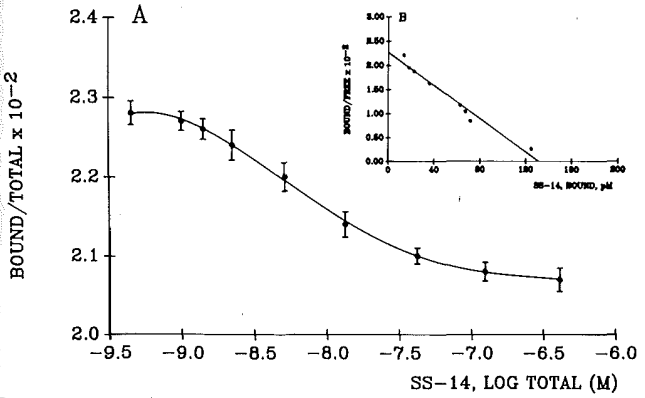

FIG. 4. A, Displacement of [^{125}I-Tyr^{11}]SS-14 by increasing amounts of unlabeled SS-14 using membranes of human pancreatic cancer. The individual *data points* represent the average value ± SE of triplicate determinations. B, Scatchard plot analysis of data from displacement curves illustrated in A. The Scatchard nonspecific bound to free ratio was 0.02114.

TABLE 3. Displacement of [^{125}I-Tyr^{11}]SS-14 with SS-14 and its analogs from membrane receptors on human and experimental pancreatic cancers and normal tissues

Tissue	Peptides (unlabeled)	K_a (nM^{-1})
Normal human pancreas	SS-14	0.34
	RC-121	0.64
	RC-160	0.44
	RC-95-I	0.22
	RC-98-I	1.33
	RC-101-I	0.04
	SMS-201-995	83.11
Human pancreatic cancer	SS-14	0.29
	RC-121	0.52
	RC-160	0.48
	RC-95-I	0.03
	RC-98-I	2.68
	RC-101-I	0.02
	SMS-201-995	0.001
MIA PaCa-2 human pancreatic cancer cell line	SS-14	0.03
	RC-121	0.01
	RC-160	0.13
	RC-95-I	ND
	RC-98-I	0.09
	RC-101-I	0.02
Normal hamsters pancreas	SS-14	0.44
	RC-121	0.14
	RC-160	1.70
	RC-95-I	0.13
	RC-98-I	0.80
	RC-101-I	0.43
BOP-induced pancreatic cancer in hamsters	SS-14	1.01
	RC-121	0.38
	RC-160	0.17
	RC-95-I	0.16
	RC-98-I	0.07
	RC-101-I	0.22

K_a, Affinity constant of ligand for membrane receptors; ND, no displacement. The results of each experiment were calculated from data of triplicate tubes of a 10-point assay. The coefficients of variations of the determination ranged from 8–24%.

lower than that of RC-121. In human prostate cancer, SS-14, RC-98-I, and RC-95-I showed the highest affinity to SS-14-binding sites. In normal human prostate, human prostate cancer, and Dunning R3327H rat prostate tumor, analog SMS-201-995 showed markedly lower affinity to SS-14 receptors than the other octapeptide analogs.

We were unable to detect receptors for SS-14 in specimens of normal human postmenopausal ovary and normal rat ovary (not shown). In normal premenopausal ovary, SS-14 was bound to receptors with low affinity (Table 5). The analysis of displacement curves of [^{125}I-Tyr^{11}]SS-14 by unlabeled SS-14 and its analogs from ovarian adenocarcinoma and arrhenoblastoma indicated

DOCKET ALARM

Explore Litigation Insights

Docket Alarm provides insights to develop a more informed litigation strategy and the peace of mind of knowing you're on top of things.

Real-Time Litigation Alerts

Keep your litigation team up-to-date with **real-time alerts** and advanced team management tools built for the enterprise, all while greatly reducing PACER spend.

Our comprehensive service means we can handle Federal, State, and Administrative courts across the country.

Advanced Docket Research

With over 230 million records, Docket Alarm's cloud-native docket research platform finds what other services can't. Coverage includes Federal, State, plus PTAB, TTAB, ITC and NLRB decisions, all in one place.

Identify arguments that have been successful in the past with full text, pinpoint searching. Link to case law cited within any court document via Fastcase.

Analytics At Your Fingertips

Learn what happened the last time a particular judge, opposing counsel or company faced cases similar to yours.

Advanced out-of-the-box PTAB and TTAB analytics are always at your fingertips.

API

Docket Alarm offers a powerful API (application programming interface) to developers that want to integrate case filings into their apps.

LAW FIRMS
Build custom dashboards for your attorneys and clients with live data direct from the court.

Automate many repetitive legal tasks like conflict checks, document management, and marketing.

FINANCIAL INSTITUTIONS
Litigation and bankruptcy checks for companies and debtors.

E-DISCOVERY AND LEGAL VENDORS
Sync your system to PACER to automate legal marketing.